J|A|C|S
ARTICLES
Published on Web 11/16/2002

C_3-Symmetrical Supramolecular Architectures: Fibers and Organic Gels from Discotic Trisamides and Trisureas

Judith J. van Gorp, Jef A. J. M. Vekemans, and E. W. Meijer*

Contribution from the Laboratory of Macromolecular and Organic Chemistry, Eindhoven University of Technology, P.O. Box 513, 5600 MB, Eindhoven, The Netherlands

Received July 18, 2002

Abstract: Hydrogen bonded C_3-symmetrical molecules that associate into supramolecular stacks are described. Structural mutation on these molecules has been performed to elucidate the contribution of the different secondary interactions (hydrogen bonding, $\pi-\pi$ stacking) to the self-assembly of the disks into chiral stacks. Twelve C_3-symmetrical molecules have been investigated, six of which contain three central amide functionalities (**1a**−**f**) and six of which contain three central urea groups (**2a**−**f**). Peripheral groups of the disks are "small", "medium", or "large", half of them being achiral and the other half being chiral, to enable investigation of the supramolecular architectures with CD spectroscopy. In all of the cases, elongated, helical stacks are formed in apolar solution, except for the "medium" amide disks **1c/d**. The elongated stacks of the C_3-symmetrical disks form gels, which are visualized by AFM and SANS, and this confirms the directionality of the interactions. For the "large" urea disk, **2f**, fibers with a length of up to 2 μm are observed. Temperature dependent and "sergeants-and-soldiers" CD measurements reveal that the urea stacks are much more rigid than the corresponding amide ones. In case of the "medium" urea disks, **2c/d**, a true rigid rod, is formed. Where amide disks immediately reach their thermodynamic equilibrium, kinetic factors seem to govern urea aggregation. In a number of experiments aimed at reversibility with the urea stacks, hysteresis is observed, implying that these urea disks initially form a poorly defined stack, which subsequently transforms slowly into a well-defined, chiral architecture.

Introduction

Self-assembly may open new possibilities in both the fields of biology and materials science because it enables the rapid formation of nanosized, complex architectures, adopting stable and compact conformations, despite their noncovalent, reversible nature.[1a−g] A vast number of these structures are known, which contain strong (self-)complementary and unidirectional intermolecular interactions to enforce one-, two-, or three-dimensional self-assembled architectures.[2a−j] The self-assembled systems have been applied in so-called organogels,[3a−n] for example, those of the well-known cyanuric acid/melamine motifs.[2a−e,3a−c] In an organogel, the liquid is prevented from flowing by a continuous, three-dimensional, entangled network of fibers of low molecular weight organogelators,[4a−b] held together solely by noncovalent forces, including hydrogen bonding, $\pi-\pi$ stacking, and solvophobic interactions. Much effort is being put into the design of new organogelators,[5a−e] but even when the basic requirements of gel formation are met (supramolecular aggregation and cross-link formation), external factors (concentration, temperature, solvent, and stoichiometry) can prevent gel formation.[6] Irreversible precipitation of fibers is induced, similar to the irreversible aggregation of proteins in case of neuro-degenerative diseases, such as Alzheimer's and Creutzfeldt−Jakob's disease.[7a−b] To increase insight into the supramolecular aggregation phenomena, the exact nature and relative importance of the secondary interactions were studied. For this purpose, discotic molecules were selected as highly suitable building blocks for the formation of cylindrically shaped fibers.[8] Both solvophobic effects and $\pi-\pi$ stacking,[9a−c] as well as hydrogen bonding,[9d,e] are used to assemble the disklike entities. Remarkably, hydrogen bonding is also used to preorganize the core of the disk,[9f,g] or even to form the disk by bringing together multiple precursors.[9h−l] Introduction of chirality in the discotics may lead to helical fibers.[9m−o] Next to the

* To whom correspondence should be addressed. E-mail: E.W.Meijer@tue.nl.

(1) Reviews: (a) Prins, L. J.; Reinhoudt, D. N.; Timmerman, P. *Angew. Chem., Int. Ed.* **2001**, *40*, 2382−2426. (b) Hill, D. J.; Mio, M. J.; Prince, R. J.; Hughes, T. S.; Moore, J. S. *Chem. Rev.* **2001**, *101*, 3893−4011. (c) Brunsveld, L.; Folmer, B. J. B.; Meijer, E. W.; Sijbesma, R. P. *Chem. Rev.* **2001**, *101*, 4071−4097. (d) Sherrington, D. C.; Taskinen, K. A. *Chem. Soc. Rev.* **2001**, *30*, 83−93. (e) Greig, L. M.; Philp, D. *Chem. Soc. Rev.* **2001**, *30*, 287−302. (f) Bong, D. T.; Clark, T. D.; Granja, J. R.; Ghadiri, M. R. *Angew. Chem., Int. Ed.* **2001**, *40*, 989−1011. (g) Ciferri, A. *Macromol. Rapid Commun.* **2002**, *23*, 511−529.

(2) Some examples of self-assembled architectures: cyanuric acid/melamine motifs: (a) Zerowski, J. A.; Seto, C. T.; Wierda, D. A.; Whitesides, G. M. *J. Am. Chem. Soc.* **1990**, *112*, 9025−9026. (b) Prins, L. J.; de Jong, F.; Timmerman, P.; Reinhoudt, D. N. *Nature* **2000**, *408*, 181−184. (c) Hof, F.; Nuckolls, C.; Rebek, J. Jr. *J. Am. Chem. Soc.* **2000**, *122*, 4251−4252. (d) Berl, V.; Huc, I.; Lehn, J.-M.; DeCian, A.; Fischer, J. *Eur. J. Org. Chem.* **1999**, 3089−3094. (e) Freeman, A. W.; Vreekamp, R.; Fréchet, J. M. J. *Polym. Mater. Sci. Eng.* **1997**, *77*, 138−140. dendritic isophthalic acid: (f) Zimmerman, S. C.; Zeng, F.; Reichert, D. E. C.; Kolotuchin, S. V. *Science* **1996**, *271*, 1095−1098. gallate-based columns: (g) Percec, V.; Ahn, C.-H.; Ungar, G.; Yeardley, D. J. P.; Möller, M.; Sheiko, S. S. *Nature* **1998**, *391*, 161−164. (h) Percec, V.; Holerca, M. N.; Uchida, S.; Cho, W.-D.; Ungar, G.; Lee, Y.; Yeardley, D. J. P. *Chem. Eur. J.* **2002**, *8*, 1106−1117. deoxyguanosine oligomers: (i) Gottarelli, G.; Proni, G.; Spada, G. P.; Bonazzi, S.; Garbesi, A.; Ciuchi, F.; Mariani, P. *Biopolymers* **1997**, *42*, 561−574. ureido pyrimidinone: (j) Beijer, F. H.; Sijbesma, R. P.; Kooijman, H.; Spek, A. L.; Meijer, E. W. *J. Am. Chem. Soc.* **1998**, *120*, 6761−6769.

10.1021/ja020984n CCC: $22.00

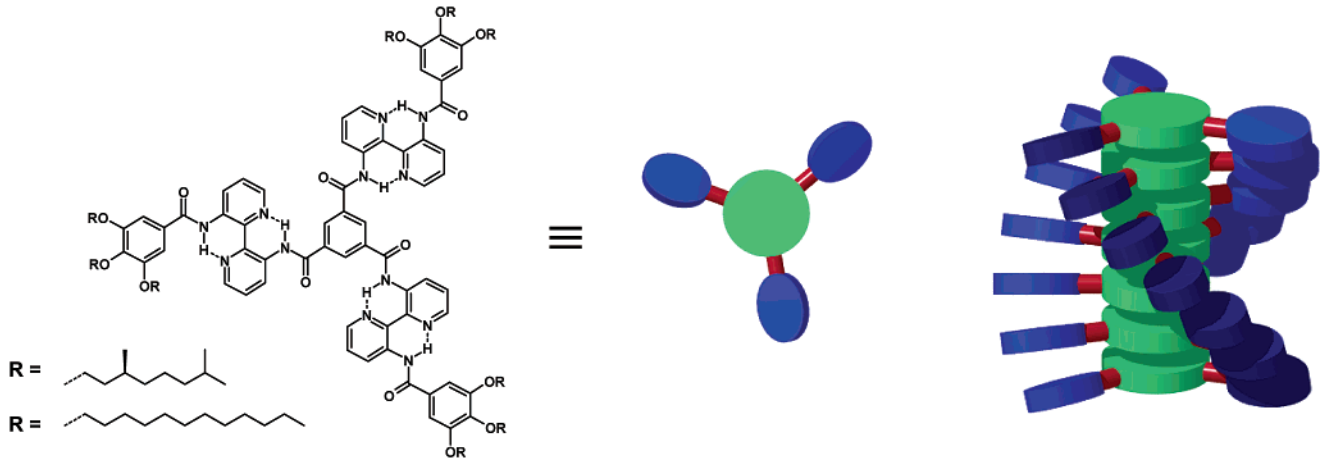

Figure 1. First bypiridine based C_3-symmetrical disks and a cartoon representing their helical supramolecular stacking.

possibility of creating cholesteric and ferrroelectric liquid crystals, chirality was recognized as a new tool in studying the self-assembly of the disks. The discotic structures cover a broad range of rotational symmetries (e. g., ranging from C_2 to C_6), but from an esthetic and practical point of view, C_3-symmetrical compounds were found to be highly attractive,[9e,g,k,l,p−r] especially those containing a 1,3,5-benzenetricarboxamide unit.[10a−c,11]

Recently, we reported on various C_3-symmetrical columnar supramolecular architectures relying on hydrogen bonding in combination with $\pi-\pi$ stacking.[11−13] The first representatives of this class of C_3-symmetrical self-assembled structures were built up convergently by the stepwise acylation of 2,2′-bipyridine-3,3′-diamine (Figure 1).[12a−d] The bipyridinyl parts are planar and preorganized due to their intramolecular hydrogen bonds; the gallic moieties are equipped with alkyl groups, inducing phase separation, whereas the assemblies feature a 3-fold array of intermolecular hydrogen bonds. Order is not only observed in the solid or liquid crystalline phase,[12a] the lyotropic organic gel phase,[12b] but also in dilute solution.[12c] Chirality in the solubilizing side chain of the constituting molecules allowed investigation of the three-dimensional structure of the aggregates using CD spectroscopy. The self-assembled stacks undergo a huge amplification of chirality,[14] with 1 chiral molecule capable of organizing as many as 80 achiral ones in either a right- or a left-handed helical stack in dilute solution. Although the cooperativity is high, the aggregation ($K = 10^8$ l/mol) is still completely reversible without displaying any hysteresis. However, enlargement of the central aromatic core with methoxy groups or pyrazine rings gives stronger but less ordered $\pi-\pi$ stacks.[12d]

(3) Some examples of low molecular weight organogelators: cyanuric acid/melamine motifs: (a) Lehn, J.-M.; Mascal, M.; DeCian, A.; Fisher, J. *J. Chem. Soc., Chem. Commun.* **1990**, 479−481. (b) Hanabusa, K.; Miki, T.; Taguchi, Y.; Koyama, T.; Shirai, H. *J. Chem. Soc., Chem. Commun.* **1993**, 1382−1384. (c) Jeong, S. W.; Murata, K.; Shinkai, S. *Supramolec. Sci.* **1996**, *3*, 83−86. anthraquinone derivatives: (d) Brotin, T.; Utermöhlen, R.; Fages, F.; Bouas-Laurent, H.; Desvergne, J.-P. *J. Chem. Soc., Chem. Commun.* **1991**, 416−418. porphyrin derivatives: (e) Tamaru, S.; Takeuchi, M.; Sano, M.; Shinkai, S. *Angew. Chem., Int. Ed.* **2002**, *41*, 853−856. cyclohexane-based bisureas: (f) van Esch, J.; Schoonbeek, F.; de Loos, M.; Kooijman, H.; Spek, A. L.; Kellogg, R. M.; Feringa, B. L. *Chem. Eur. J.* **1999**, *5*, 937−950. (g) Hanabusa, K.; Shimura, K.; Hirose, K.; Shirai, H. *Chem. Lett.* **1996**, 885−886. linear bisureas: (h) Shi, C.; Huang, Z.; Kilic, S.; Xu, J.; Enick, R. M.; Beckman, E. J.; Carr, A. J.; Melendez, R. E.; Hamilton, A. D. *Science* **1999**, *286*, 1540−1543. cyclic amides: (i) Hanabusa, K.; Matsumoto, Y.; Miki, T.; Koyama, T.; Shirai, H. *J. Chem. Soc., Chem. Commun.* **1994**, 1401−1402. cyclohexane based bisamides: (j) Hanabusa, K.; Yamada, M.; Kimura, M.; Shirai, H. *Angew. Chem., Int. Ed. Engl.* **1996**, *35*, 1949−1951. α-amino acid derivatives: (k) Partridge, K. S.; Smith, D. K.; Dykes G. M.; McGrail, P. T. *Chem. Commun.* **2001**, 319−320. amino sugars: (l) Yoza, K.; Amanokura, N.; Ono, Y.; Akao, T.; Shinmori, H.; Takeuchi, M.; Shinkai, S.; Reinhoudt, D. N. *Chem. Eur. J.* **1999**, *5*, 2722−2729. (m) Hafkamp, R. H.; Feiters, M. C.; Nolte, R. J. M. *J. Org. Chem.* **1999**, *64*, 412−426. sugars: (n) Sakurai, K.; Kimura, T.; Gronwald, O.; Inoue, K.; Shinkai, S. *Chem. Lett.* **2002**, 746−747.

(4) (a) Flory, P. J. *Faraday Discuss. R. Soc. Chem.* **1974**, *57*, 7−18. (b) Tanaka, T. *Am. Sci.* **1981**, *244*, 110−123.

(5) (a) van Esch, J. H.; Feringa, B. L. *Angew. Chem., Int. Ed.* **2000**, *39*, 2263−2266. (b) Schoonbeek, F. S. *Thesis: Making it all stick together*; University of Groningen: Groningen, 2001. (c) Lucas, L. N. *Thesis: Dithienylcyclopentene optical switches*; University of Groningen: Groningen, 2001. (d) Terech, P.; Weiss, R. *Chem. Rev.* **1997**, *97*, 3133−3159. (e) Luboradzki, R.; Gronwald, O.; Ikeda, M.; Shinkai, S.; Reinhoudt, D. N. *Tetrahedron* **2000**, *56*, 9595−9599.

(6) Berl, V.; Schmutz, M.; Krische, M. J.; Khoury, R. G.; Lehn, J.-M. *Chem. Eur. J.* **2002**, *8*, 1227−1244.

(7) (a) Tranchant, C.; Rodier, G.; Schmitthaeusler, R.; Warren, J. M. *Rev. Neurol.* **1996**, *152*, 153−157. (b) Buxbaum, J. N.; Tagoe, C. E. *Annu. Rev. Med.* **2000**, *51*, 543−569.

(8) Chandrasekhar, S.; Sadashiva, B. K.; Suresh, K. A. *Pramana* **1977**, *9*, 471−480.

(9) $\pi-\pi$ Stacked disks: (a) Tobe, Y.; Utsumi, N.; Kawabata, K.; Nagano, A.; Adachi, K.; Araki, S.; Sonoda, M.; Hirose, K.; Naemura, K. *J. Am. Chem. Soc.* **2002**, *124*, 5350−5364. (b) Lahiri, S.; Thompson, J. L.; Moore, J. S. *J. Am. Chem. Soc.* **2000**, *122*, 11 315−11 319. (c) Höger, S.; Bonrad, K.; Mourran, A.; Beginn, U.; Möller, M. *J. Am. Chem. Soc.* **2001**, *123*, 5651−5659. H-bonded disks: (d) Percec, V.; Ahn, C. H.; Bera, T. K.; Ungar, G.; Yeardley, D. J. P. *Chem. Eur. J.* **1999**, *5*, 1070−1083. (e) Bushey, M. L.; Hwang, A.; Stephens, P. W.; Nuckolls, C. *Angew. Chem., Int. Ed.* **2002**, *41*, 2828−2831. H-bond stabilized disks: (f) Paulus, W.; Ringsdorf, H.; Diele, S.; Pelzl, G. *Liq. Cryst.* **1991**, *9*, 807−819. (g) Shu, W.; Valiyaveettil, S. *Chem. Commun.* **2002**, 1350−1351. (h) Kleppinger, R.; Lillya, P.; Yang, C. *J. Am. Chem. Soc.* **1997**, *119*, 4097−4102. (i) Yang, W.; Chai, X.; Chi, L.; Liu, X.; Cao, Y.; Lu, R.; Jiang, Y.; Tang, X.; Fuchs, H.; Li, T. *Chem. Eur. J.* **1999**, *5*, 1144−1149. (j) Beginn, U.; Sheiko, S.; Möller, M. *Macromol. Chem. Phys.* **2000**, *201*, 1008−1015. (k) Suárez, M.; Lehn, J.-M.; Zimmerman, S. C.; Skoulios, A.; Heinrich, B. **1998**, *120*, 9526−9532. (l) Kraft, A.; Reichert, A.; Kleppinger, R. *Chem. Commun.* **2000**, 1015−1016. chiral disks: (m) Fechtenkötter, A.; Tchebotareva, N.; Watson, M.; Müllen, K. *Tetrahedron* **2001**, *57*, 3769−3783. (n) Engelkamp, H.; Middelbeek, S.; Nolte, R. J. M. *Science* **1999**, *284*, 785−788. (o) Tamaru, S.; Uchino, S.; Takeuchi, M.; Ikeda, M.; Hatano, T.; Shinkai, S. *Tetrahedron Lett.* **2002**, *43*, 3751−3755. C_3- symmetrical disks: (p) Boden, N.; Bushby, R. J.; Hardy, C.; Sixl, F. *Chem. Phys. Lett.* **1986**, *123*, 359−364. (q) Pieterse, K.; van Hal, P. A.; Kleppinger, R.; Vekemans, J. A. J. M.; Janssen, R. A. J.; Meijer, E. W. *Chem. Mater.* **2001**, *13*, 2675−2679. (r) Yasuda, Y.; Takebe, Y.; Fukumoto, M.; Inada, H.; Shirota, Y. *Adv. Mater.* **1996**, *8*, 740−741.

(10) (a) Yasuda, Y.; Iishi, E.; Inada, H.; Shirota, Y. *Chem. Lett.* **1996**, 575−576. (b) Hanabusa, K.; Koto, C.; Kimura, M.; Shirai, H.; Kakehi, A. *Chem. Lett.* **1997**, 429−430. (c) Matsunaga, Y.; Miyajima, N.; Nakayasu, Y.; Sakai, S. *Bull. Chem. Soc. Jpn.* **1988**, 61, 207−210.

(11) Brunsveld L.; Schenning, A. P. H. J.; Broeren, M. A. C.; Janssen, H. M.; Vekemans, J. A. J. M.; Meijer, E. W. *Chem. Lett.* **2000**, 292−293.

(12) (a) Palmans, A. R. A.; Vekemans, J. A. J. M.; Fischer, H.; Hikmet, R. A.; Meijer, E. W. *Chem. Eur. J.* **1997**, *3*, 300−307. (b) Palmans, A. R. A.; Vekemans, J. A. J. M.; Hikmet, R. A.; Fisher, H.; Meijer, E. W. *Adv. Mater.* **1998**, *10*, 873−876. (c) Palmans, A. R. A.; Vekemans, J. A. J. M.; Havinga, E. E.; Meijer, E. W. *Angew. Chem., Int. Ed. Engl.* **1997**, *36*, 2648−2651. (d) Meijer, E. W.; Vekemans, J. A. J. M.; Palmans, A. R. A.; Breure, P.; de Kraker, J.; Brunsveld, L. *Polym. Prepr.* **2000**, *41*, 902−903.

(13) Brunsveld, L.; Zhang, H.; Glasbeek, M.; Vekemans, J. A. J. M.; Meijer, E. W. *J. Am. Chem. Soc.* **2000**, *122*, 6175−6182.

(14) Green, M. M.; Reidy, M. P.; Johnson, R. D.; Darling, G.; O'Leary, D. J.; Wilson, G. *J. Am. Chem. Soc.* **1989**, *111*, 6452−6454.

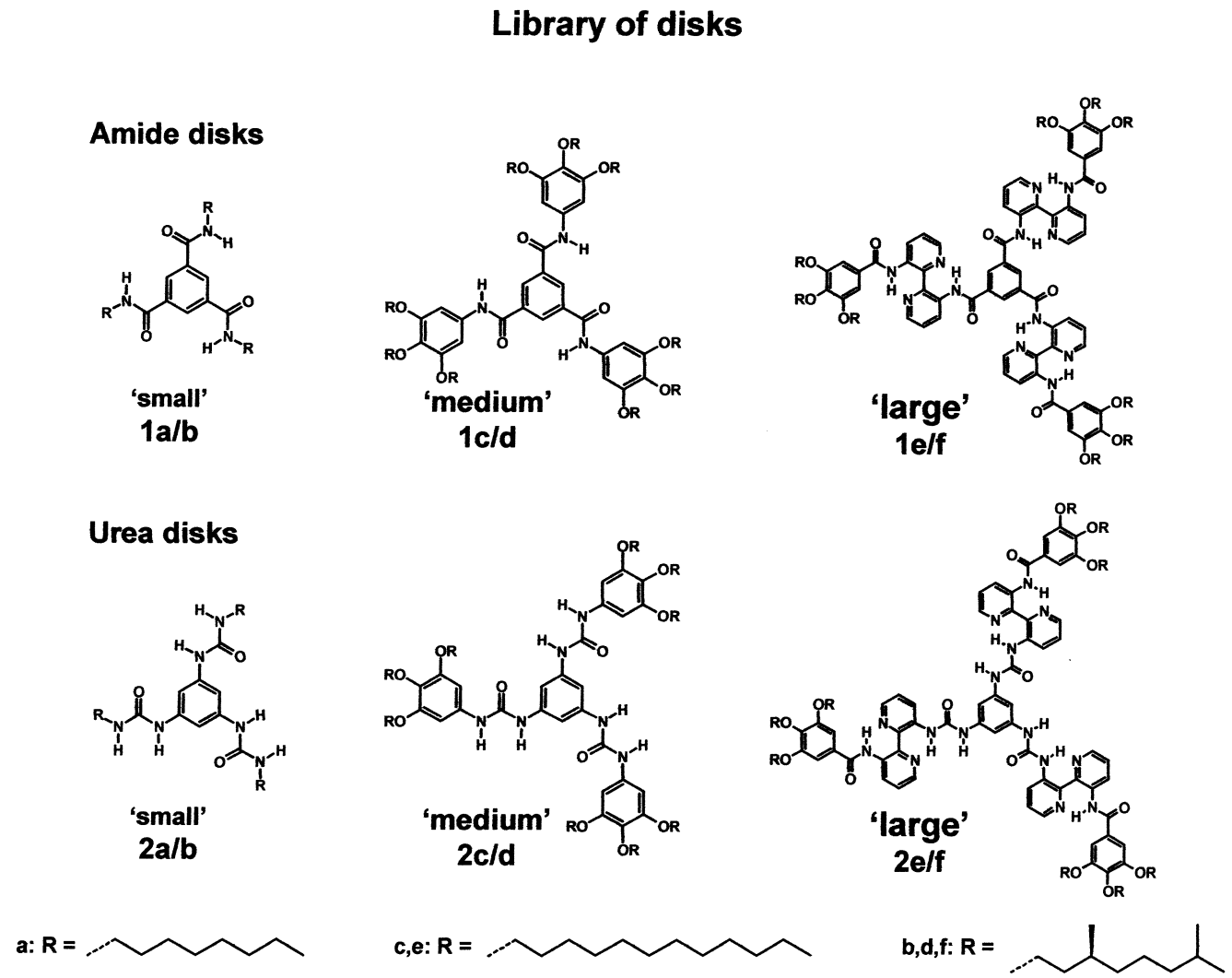

Figure 2. Overview of twelve C_3-symmetrical disks, containing central amides (**1a**−**f**) or ureas (**2a**−**f**). The peripheral groups of the disks are "small" (**1a/b** and **2a/b**), "medium" (**1c/d** and **2c/d**) or "large" (**1e/f** and **2e/f**). Half of the disks are achiral (**1a/c/e** and **2a/c/e**); the other half is chiral (**1b/d/f** and **2b/d/f**).

To what extent both intermolecular hydrogen bonding and $\pi-\pi$ interactions contribute to the cooperative, helical self-assembly is an intriguing question. That both secondary interactions play a role was elucidated by the stepwise growth of analogous disks equipped with oligo(ethylene oxide) tails into chiral columns in polar media.[13] First, achiral, small aggregates are generated by the hydrophobicity of the core. Second, the expression of the more sensitive hydrogen bonding interactions gives rise to large, chiral, self-assembled structures. In apolar media, with hydrophobic peripheral tails, such a stepwise aggregation does not occur and both secondary interactions are proposed coming to expression simultaneously.

To unravel the features governing self-assembly in apolar media, several $\pi-\pi$ interacting groups and hydrogen bonding units have been combined to afford a series of C_3-symmetrical disks (Figure 2). The $\pi-\pi$ interactions were increased by replacing "small" alkyl tails (**1a/b**, **2a/b**) by "medium" gallic groups (**1c/d**, **2c/d**) or "large" bipyridinyl-gallic groups (**1e/f**, **2e/f**). The intermolecular hydrogen bonding amide moieties in **1a**−**f** were substituted by urea ones in **2a**−**f**. Because a urea has two protons to form hydrogen bonds, whereas an amide has only one, the urea bond is considered stronger and more rigid. In this paper, we compare the behavior of twelve C_3-symmetrical disks. Previously, the supramolecular properties of **1a/b**[10a−c, 11] and **1e/f**[12a−d] have been described, all of the other members of the library are novel.

Results

Synthesis. Trisamides **1a**−**f** are formed by 3-fold reaction of trimesyl chloride with amines **3a**−**f**, of which the chiral ones **3b**,[15] **3d**,[16] and **3f**[12a−d] are based on the (*S*)-3,7-dimethyloctyl unit (Scheme 1). The syntheses of compounds **1a/b** and **1e/f** have been described before.[11,12a−d] Trisamides **1c** and **1d** are obtained in reasonable yield after column chromatography (86% and 70% for **1c** and **1d**, respectively). The trisureas **2a**−**f** are obtained by 3-fold reaction of amines **3a**−**f** with 1,3,5-benzenetriisocyanate (**5**). The latter is synthesized in 90% yield by treatment of trimesyl chloride with sodium azide, and subsequent thermolysis of trimesyl azide (**4**)[17] to induce the Curtius rearrangement.[18] The urea disks are obtained in satisfac-

(15) Fontana, M.; Chanzy, H.; Caseri, W. R.; Smith, P.; Schenning, A. P. H. J.; Meijer, E. W.; Gröhn, F. *Chem. Mater.* **2002**, *14*, 1730−1735.
(16) Pieterse, K. *Thesis: Electron deficient materials based on azaheterocycles*; Technische Universiteit Eindhoven: Eindhoven, 2001.
(17) Trimesyl azide (**4**) is explosive under heat or pressure in the solid state.
(18) Ambade, A. V.; Kumar, A. *J. Polym. Sci., Part A: Polym. Chem.* **2001**, *39*, 1295−1304.

Scheme 1. Synthesis of Disk Shaped Amides **1a**−**f** and Ureas **2a**−**f**

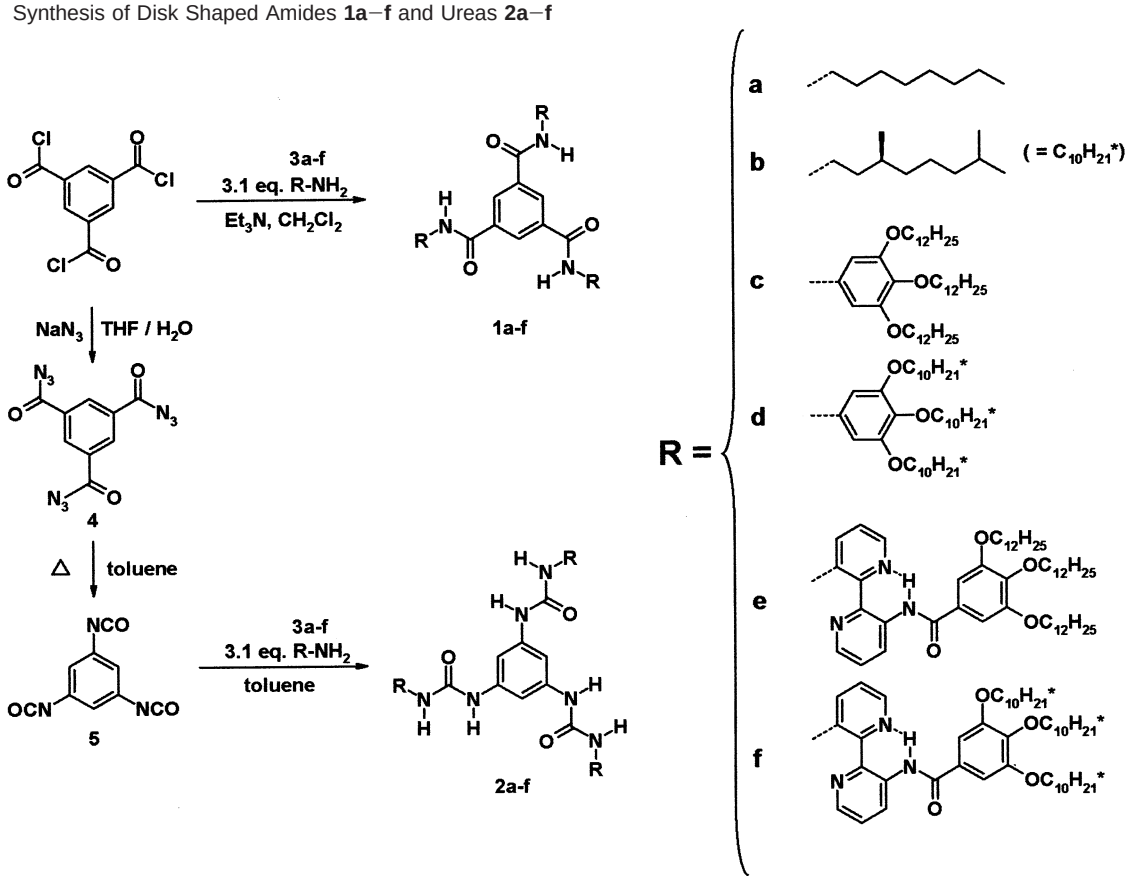

tory yield after washing with the appropriate solvent (yields for **2a**, 70%; **2b**, 68%; **2c**, 87%; **2d**, 78%; **2e**, 75%; and **2f**, 87%). All of the compounds are characterized with ^{1}H NMR, ^{13}C NMR, and IR spectroscopy, MALDI-TOF mass spectrometry and/or elemental analysis. Details on synthesis and characterization are given in the Supporting Information.

Behavior of the Pure Compounds. Optical Polarizing Microscopy and Differential Scanning Calorimetry. All of the C_3-symmetrical amide disks, **1a**−**f**, show liquid crystallinity, most of them over a broad temperature range (Table 1). Optical microscopy and DSC of the achiral "medium" compound **1c** shows that the temperature range of liquid crystallinity expands from −4 °C (44 kJ/mol) to 178 °C (27 kJ/mol). Several phases are found, indicated by the small ordered/disordered transitions at 61 °C (4.2 kJ/mol) and 96 °C (2.1 kJ/mol). In case of the chiral compound **1d** a small (<1 kJ/mol) crystalline−crystalline transition is found at lower temperatures (0 °C). Compound **1d** enters the liquid crystalline phase at 96 °C (1.8 kJ/mol) and becomes already isotropic at 113 °C (15 kJ/mol). Typical focal conic structures are found for the amide disks **1a**−**f**, pointing to a helical columnar structure (Figure 3).

The disk shaped ureas **2a**−**f** are difficult to study in the pure form, due to degradation of these compounds at temperatures around 190 °C, which is lower than the isotropization temperature. However, infrared spectroscopy shows that hydrogen bonding occurs in the ordered (liquid) crystalline phases (Table 2), indicated by the typically low positions of the carbonyl vibrations.[10a/b]

Gelation. A property inherent to the presence of elongated, columnar stacks is the possibility of forming macroscopic organogels. These gels were made by dissolving the compound in an apolar solvent by heating and subsequent cooling. When the jar could be inverted without product movement, the substance was judged a gel. Minimal gel concentrations were determined by this method (Table 3). "Medium" amide disk **1c** is not able to form a gel in apolar solvents. The trisureas **2** generally need lower minimal concentrations than the corresponding amides **1**; the "small" urea compound **2a** performs especially well in this respect.

Macroscopic order of the "large" disk shaped molecules **1e/f** and **2e/f** in the gel was proven by their birefringence in optical microscopy. In birefringent solutions of "large" amide disks **1e** in concentrations varying from 56 mg/mL (2.9×10^{-2} M) to 207 mg/mL (0.11 M) an N_c phase is present. Concentrated samples (407 mg/mL, 0.21 M) show hexagonal packing of the columns as well as a helical superstructure, indicating a D_{ho} phase.[19] For the urea disks, both in case of the achiral compound **2e** (17 mg/mL, 6.2×10^{-3} M) and chiral compound **2f** (57

Table 1. Transition Temperatures *T* [°C] and Corresponding Enthalpies Δ*H* [kJ/mol] of Disk Shaped Amides **1a**−**f**[a]

compd	K	*T* (Δ*H*)	M	*T* (Δ*H*)	I
1a[b]	•	102 (*19*)	•	204 (*17*)	•
1b[c]	•	119 (*16*)	•	236 (*21*)	•
1c	•	−4 (*44*)	•	178 (*27*)	•
1d	•	96 (*1.8*)	•	113 (*15*)	•
1e[d]	•	9 (*56*)	D_{ho}	355 (*27*)[f]	•
1f[d]	—[e]	—	D_{ho}	373 (*28*)[f]	•

[a] • = phase is observed; − = phase is not observed; K = crystalline phase; M = unidentified mesophase; D_{ho} = hexagonally ordered columnar phase; I = isotropic phase. [b] Reference 10c. [c] Reference 11. [d] Reference 19. [e] Cooling the sample down to −80 °C did not show any transition. [f] The clearing is accompanied by some decomposition of the sample making the calculated enthalpies less reliable.

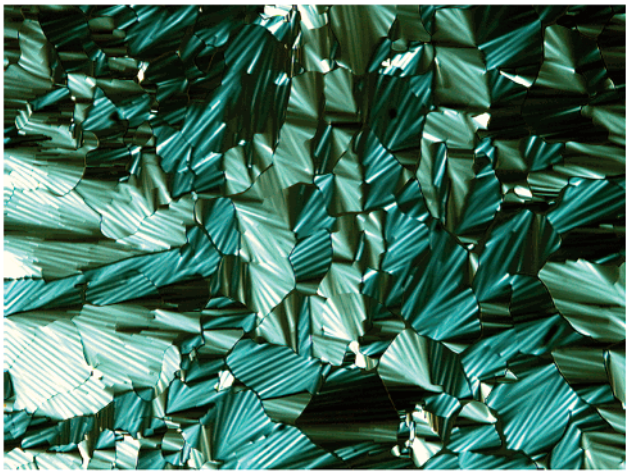

Figure 3. Typical focal conic structure found in the liquid crystalline phase for achiral "medium" amide disk **1c**.

Table 2. Wavenumbers σ [cm^{-1}] of the Carbonyl Stretch Vibrations of Amides **1a**−**f** and Ureas **2a**−**f** in the Solid State

compd	**1a**[a]	**1c**	**1e**[b]
	1640	1682	1668
solid state		1664	
compd	**2a**	**2c**	**2e**
	1632	1641	1670
solid state			1623

[a] Reference 20. [b] Reference 19.

Table 3. Minimal Gel Concentrations (concentration [mg/mL]; concentration [M]; solvent) of Amides **1a**−**f** and Ureas **2a**−**f**

	amide (**1**)	urea (**2**)
"small" (**a**)	55 mg/mL[a] 8.8×10^{-2} M hexane	1.2 mg/mL 2.0×10^{-3} M toluene
"medium" (**c**)		174 mg/mL 8.1×10^{-2} M heptane
"large" (**e**)	37 mg/mL[b] 1.4×10^{-2} M dodecane	17 mg/mL 6.2×10^{-3} M dodecane

[a] **1b** in reference 10b. [b] Reference 19.

mg/mL, 2.3×10^{-2} M), focal conic structures were found in dodecane, indicative of a columnar phase.

Macroscopic gelation is supposed to be the result of a network of fibers present in apolar solutions of amides **1a/b** and **1e/f** or ureas **2a**−**f**. For the "medium" and "large" molecules **1/2c**−**f** this network can be visualized by atomic force microscopy (AFM) and small angle neutron scattering (SANS). With these techniques, the dimensions of the aggregates can also be verified. The cross sections of the amide and urea molecules should be almost equal. For the "large" amides **1f** an interdisk distance[21] of 3.5 Å and an intercolumn distance of 38 Å were calculated from X-ray diffraction.[19] In case of the "medium" and "large"

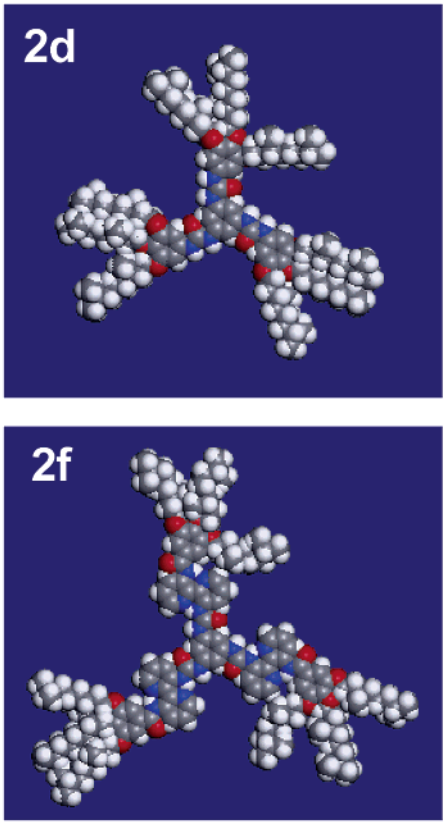

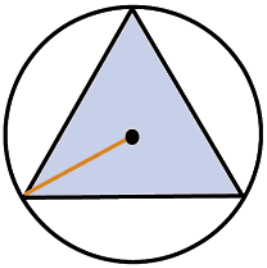

Figure 4. CPK models of "medium" **2d** (upper model) and "large" **2f** (lower model) urea disks. The blue triangle represents the aromatic core of the disks (the area looking gray (carbon), red (oxygen) and blue (nitrogen) in the CPK models); the orange line represents the radius of this aromatic core.

urea disks **2d** and **2f**, a CPK model of the molecule was used to derive the radius of the aromatic core (Figure 4). A radius of 9.8 Å was calculated for the "medium" urea disk and of 16 Å for the "large" urea disk. Reasonably, the total cross section of the molecule is somewhat smaller than twice this radius. On the other hand, some extra space has to be accounted for the alkyl tails. In summary, with both AFM and SANS, cross sections of about 20 Å for "medium" urea **2d** and 32−38 Å for "large" urea **2f** should be found.

Atomic Force Microscopy. For the "medium" amide **1d**, no network was found (Figure 5). This was expected, in view of the absence of a viscous solution. By contrast, the trisurea molecules **2d** and **2f** did show gel formation, and a network of fibers was observed in the AFM scans, indeed. In case of the "large" urea **2f**, the lengths of the fibers are as large as 2 μm. With an interdisk distance of 3.5 Å, this would correspond to columns consisting of as much as 5700 molecules!

Formation of the network occurs via physical cross-link points. At these points, several strands that are lying next to

(19) Palmans, A. R. A. *Thesis: Supramolecular structures based on the intramolecular H-bonding in the 3,3′-di(acylamino)-2,2′-bipyridine unit*; Technische Universiteit Eindhoven: Eindhoven, 1997.
(20) Brunsveld, L. *Thesis: Supramolecular chirality, from molecules to helical assemblies in polar media*; Technische Universiteit Eindhoven: Eindhoven, 2001.
(21) Interdisk distance: distance between two superimposed central aryl units of two disks in one column; intercolumn distance: lateral distance between the centers of two coplanar columns.

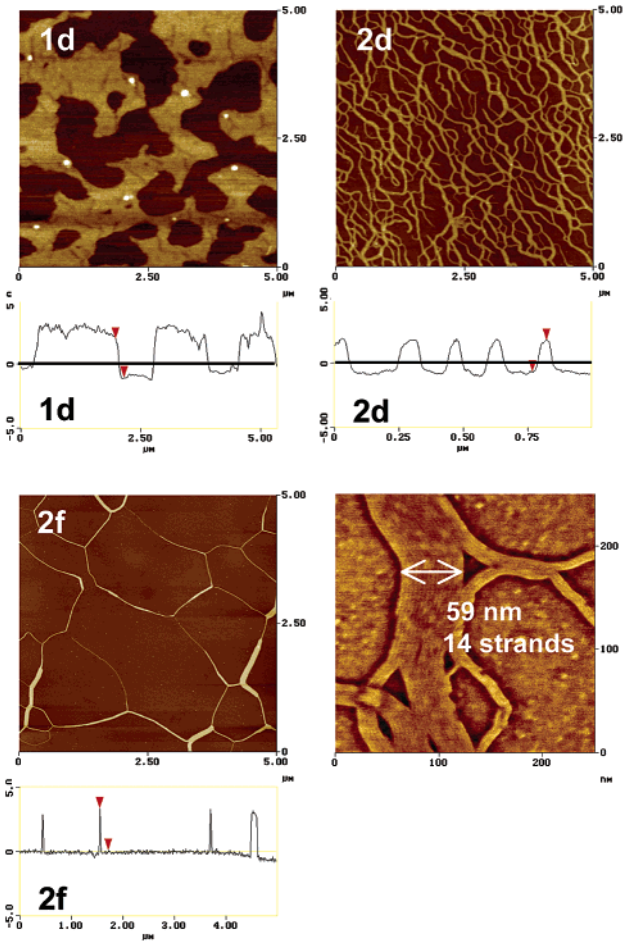

Figure 5. AFM pictures and height profiles of "medium" amide disk **1d** (top left), "medium" urea disk **2d** (top right) and "large" urea disk **2f** (bottom left) as well as a physical cross-link point of "large" urea disk **2f** (bottom right).

Table 4. Cross Sections [Å] of "medium" Urea **2d**, "large" Urea **2f** and "large" Amide **1f** Determined with Different Techniques

	CPK	AFM (height)	AFM (width)	SANS
"medium" (**2d**)	20	22		33
"large" (**2f**)	32	32	42	39
			X-ray	
"large" (**1f**)[a]	28		38	

[a] Reference 19.

each other split up and continue separately, to rejoin some other strands later on (Figure 5). In an area where several strands are aligned in a parallel fashion, the width of one strand can be estimated by dividing the total width by the number of strands. In this way, a width of 4.2 nm is calculated (Table 4).

However, the height profile of the structures can also be considered (Figure 5). For the "medium" amide **1d**, the height of the plateaus (3.1 nm) is constant over the sample, although no special architecture is formed. The heights of the "medium" and "large" urea fibers **2d** and **2f** are 2.2 and 3.2 nm. As expected, the smaller molecule displays the smallest height.

Small Angle Neutron Scattering. A technique for investigating the shape and dimensions of aggregates in the actual solution is small angle neutron scattering (SANS). In the plot of the scattering vector against the scattering intensity, the combination of a linear curve with a slope of −1 (in the intermediate angle area) with a symmetrical side maximum (in the large angle area) indicates the presence of cylindrical aggregates. Indeed, this situation applies to 6 mg/mL solutions of the "medium" and "large" urea disks **2d** and **2f** in dodecane-*d26*, in which case the length of the aggregate is at least 150 nm (Figure 6). At very low scattering vectors, the curve of "medium" urea **2d** positively deviates from linearity. Because these systems reveal thermo-reversible gel formation, this deviation must be attributed to the presence of columnar clusters that represent the physical cross-links in the gel. From the position of the side maximum, the radius of the cross section "R_c" can be determined using the formula "$R_c \approx 4.48/q_{max}$". The cross section of the "large" urea disk **2f** (39 Å) is indeed larger than that of the "medium" one **2d** (33 Å).

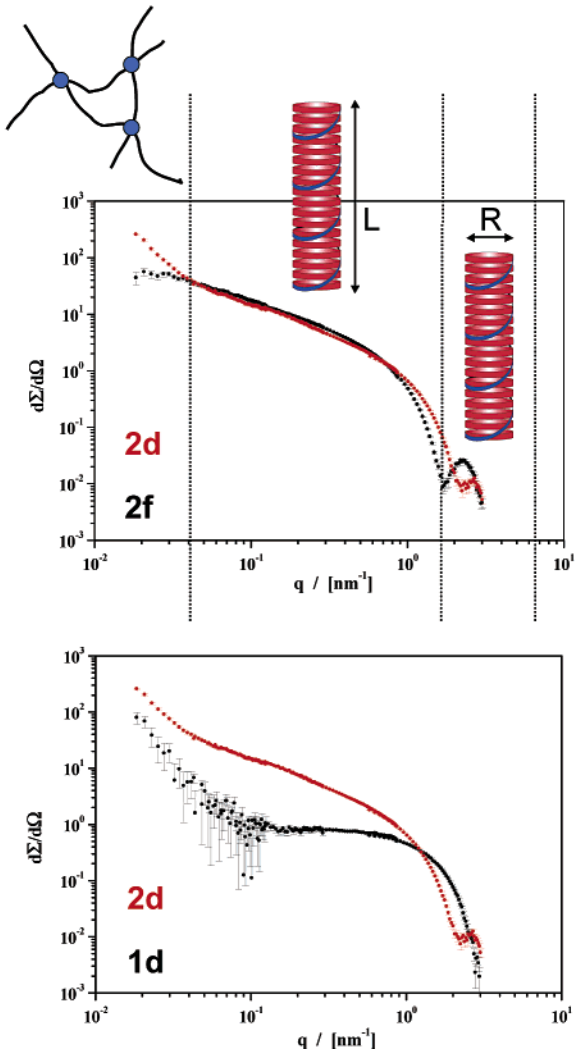

Figure 6. SANS data of "medium" urea disk **2d** (red line), "large" urea disk **2f** (top black line) and "medium" amide disk **1d** (bottom black line).

Finally, "medium" amide disk **1d** is investigated as a reference (Figure 6). In contrast to the "medium" urea disk **2d** no linear curve with a slope of −1, and no side maximum are observed. Obviously, in this case, no elongated stacks are formed.

Infrared Spectroscopy. For "small" and "large" amide disks **1a** and **1e,** it is obvious from different techniques, such as IR and NMR spectroscopy, that intermolecular hydrogen bonding—and hence aggregation—remains present in (dilute) apolar solutions, whereas for "medium" amide disks **1c**, this is not

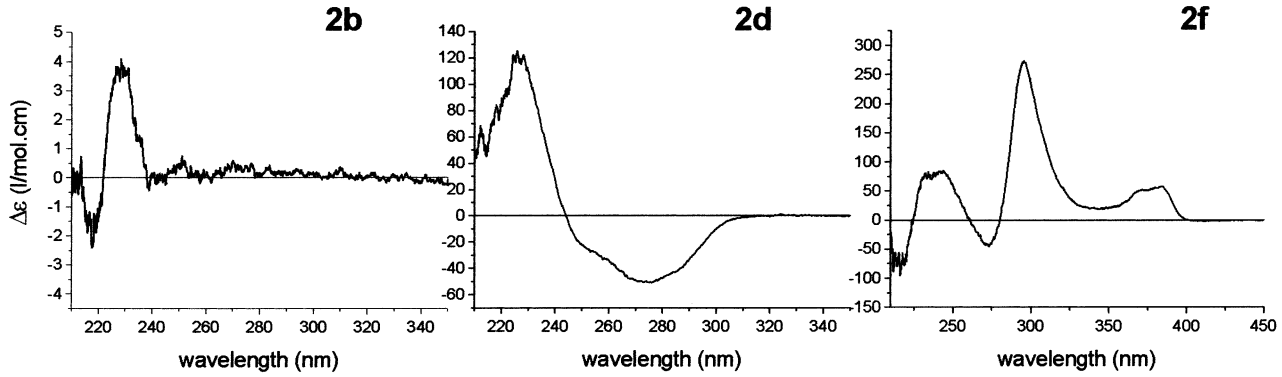

Figure 7. CD spectra of "small" **2b** (left), "medium" **2d** (middle) and "large" **2f** (right) urea disks (**2b**: 10^{-4} M in heptane, **2d**: 10^{-5} M in dodecane, **2f**: 10^{-5} M in heptane).

Table 5. Wavenumbers σ [cm^{-1}] of the Carbonyl Stretch Vibrations of Amides **1a**−**f** and Ureas **2a**−**f** in 10^{-4} M Heptane Solution

compd	**1a**[a]	**1c**	**1e**
σ	1640	1670	1669
10^{-4} M heptane		1650	
compd	**2a**	**2c**	**2e**
σ	1736	1641	1670
10^{-4} M heptane			1624

[a] Reference 20.

the case. IR gave two carbonyl vibrations in both the solid state (1682 and 1664 cm^{-1}, Table 2) and in heptane solution (1670 and 1650 cm^{-1}, Table 5), indicating the presence of both hydrogen-bonded and mono-molecular species. On the other hand, for urea disks **2c** and **2e**, the positions of the single carbonyl vibration were similar in the solid state and in 10^{-4} M heptane solution, indicating hydrogen bonding and aggregation in solution. "Small" urea **2a** is only sparingly soluble in heptane (10^{-3} M, 40 °C) and shows a carbonyl vibration that is significantly higher in heptane than in the solid state (1736 vs 1632, respectively). However, in toluene, a 10^{-4} M solution gives a similar NH stretch vibration as that found in the solid state (3285 vs 3295 cm^{-1}, respectively).

UV−Vis and Circular Dichroism Studies. To investigate the supramolecular chirality of the aggregates, the chiral disks were studied in dilute, apolar solution with CD spectroscopy. Where both "small" and "large" chiral amide disks **1b** and **1f** show significant Cotton effects, no Cotton effects were found in 10^{-4} and 10^{-5} M solutions of **1d** (or mixtures of **1c** and **1d**) in heptane. Similarly, the "small" (**2b**), "medium" (**2d**) and "large" (**2f**) urea disks were investigated (Figure 7). In contrast to the substantial Cotton effects shown by "medium" and "large" urea disks **2d** and **2f**, the effect produced by the "small" urea **2b** is only marginal (Table 6). Notable is the sign inversion between the amide and urea molecules **1f** and **2f**, despite the fact that they are based on the same side chain, with the same (*S*)-configuration of the (*S*)-3,7-dimethyloctyl group.

Temperature-Dependent Circular Dichroism Studies. To better understand the behavior of the C_3-symmetrical amide (**1a**−**f**) and urea (**2a**−**f**) molecules, temperature-dependent measurements are performed emphasizing the different maxima of the Cotton effects. The Cotton effects of "small" amide **1b**, "large" amide **1f** and "small" urea **2b** gradually decrease upon raising the temperature until they disappear at approximately

Table 6. UV and CD Data of Chiral Amides **1b/d/f** and Ureas **2b/d/f**; λ_{Max} [nm] = the Absorption Band Most toward the Red and $\epsilon/\Delta\epsilon$ [L/Mol.cm] = the Intensity of the Signal[a]

	UV–Vis		CD	
compd	λ_{max}	ϵ	λ_{max}	$\Delta\epsilon$
1b[b]	<210	9.2×10^3	224	−25.1
1d	308	2.1×10^4		
1f[c]	364	3.2×10^4	369	−23.6
	384	2.3×10^4	387	−35.6
	UV–Vis		CD	
compd	λ_{max}	ϵ	λ_{max}	$\Delta\epsilon$
2b	224	7.4×10^3	228	+3.70
2d	256	6.0×10^4	275	−51.5
2f	357	3.1×10^4	371	+52.5
	375	2.4×10^4	384	+57.4

[a] **1b**, **1d** and **2f** measured in heptane at ~10^{-5} M; **1f** and **2d** measured in dodecane at ~10^{-5} M; **2b** measured in heptane at ~10^{-4} M. [b] Reference 11 and 20. [c] Reference 19.

Table 7. Temperature-Dependent CD Data of Amides **1b/d/f** and Ureas **2b/d/f**; T [°C] = Temperature of Disappearance of the Cotton Effect; Hysteresis Indicates Whether Kinetic Factors Influence the System during Sample Preparation and Measurements[a]

compd	**1b**[b]	**1d**	**1f**[c]
T	90		110
hysteresis	no		no
compd	**2b**	**2d**	**2f**
T	100	135	80
hysteresis	no	yes	yes

[a,b,c] See the footnotes of Table 6.

100 °C (Table 7). These systems also respond immediately to changes in temperature. Upon cooling, the signal is restored at once. The "medium" urea **2d** shows a different behavior (Figure 8). The structure is retained up to very high temperatures (135 °C). At 120 °C, still one-third of the original Cotton effect is present, after which the rest is lost in a sharp transition. In case of the "large" urea disk **2f**, an even sharper transition is observed at 75 °C. The "medium" urea disk **2d** shows strong hysteresis. Upon cooling, it takes 2 days before the original signal is retrieved, while the hysteresis only takes 1.5 h for **2f**.

Comparing and Mixing Compounds. Need for C_3-Symmetry: Mono-, Di-, and Tri-Urea. From the measurements described above, we assume that the chiral aggregates of the urea disks are helical stacks, similar to the amide stacks. In a helical stack, all three wedges of the molecule are involved in

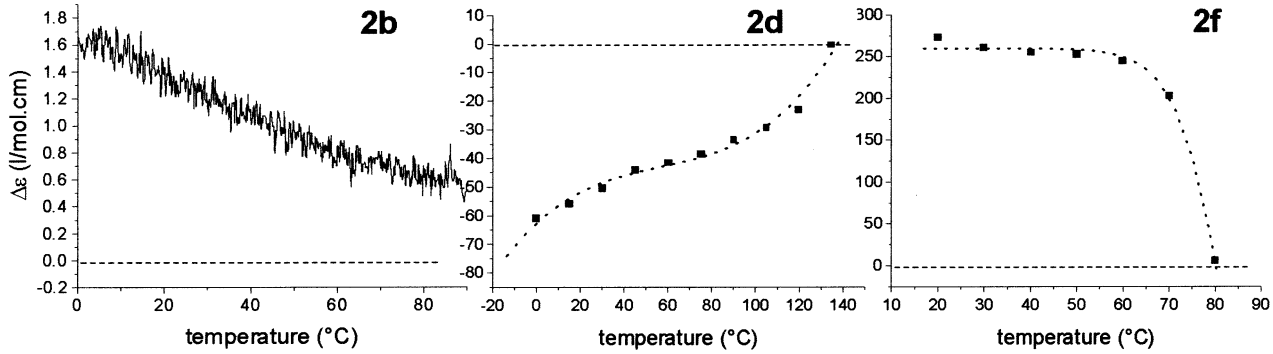

Figure 8. Temperature-dependent CD spectra of "small" **2b** (left), "medium" **2d** (middle) and "large" **2f** (right) urea disks at $\lambda_{max} = 228$, 275 and 295 nm, respectively (**2b**: 10^{-4} M in heptane, **2d**: 10^{-5} M in dodecane, **2f**: 10^{-5} M in heptane).

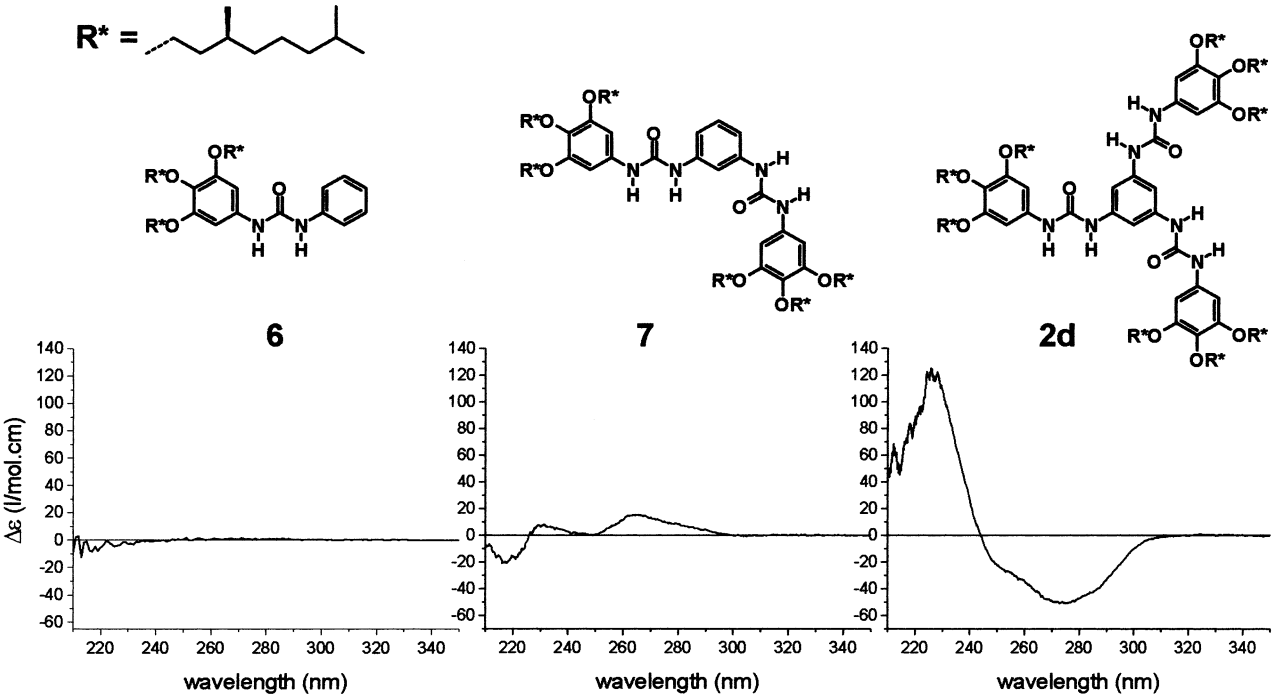

Figure 9. Chemical structures and CD spectra of "medium" mono-urea **6** (left), di-urea **7** (middle) and tri-urea **2d** (right) (10^{-5} M in heptane for **6** and **7** and in dodecane for **2d**).

formation of the supramolecular structure. To prove that this is indeed the case, we investigated a mono-urea (**6**) and a di-urea (**7**) as reference compounds for the "medium" urea disk **2d**. The CD spectrum of the mono-urea **6** shows no Cotton effect (Figure 9). The di-urea **7** does show a nice Cotton effect, but it is much smaller than that of the tri-urea **2d** and differs in shape, sign and maxima.

More differences between the di-urea **7** and tri-urea **2d** become clear when inspecting the temperature-dependent CD spectra (Figure 10). In the first place, the di-urea (80 °C) is less stable upon raising temperature than the tri-urea (135 °C). Furthermore, upon heating, the loss of signal occurs more gradually, whereas upon cooling, the signal of the di-urea is restored immediately, in contrast with that of the tri-urea, which displays a hysteresis of 2 days.

"Sergeants-and-Soldiers" Measurements. Both "small" and "large" amide disks **1a/b** and **1e/f** show a strong amplification of chirality, with one chiral molecule capable of organizing as much as 200 and 80 achiral ones, respectively, in either a right- or a left-handed helical stack. These results are interpreted as being the result of both a strong cooperative effect in the stacking and of the columns of achiral disks being inherently chiral. The insertion of a seed of chiral disk to equal amounts of P and M helix of the achiral disks induces a strong preference of one helicity over the other.

In the "large" ureas **2e/f** no "sergeants-and-soldiers" effect could be observed (Table 8). Several methods of sample preparation were applied (mixing of two solutions, heating and cooling of samples, premixing of two solids), but in all cases, a linear relationship between the intensity of the Cotton effect and the percentage of chiral molecules was observed. "Medium" ureas **2c/d** did give an amplification of 2 when the sample was prepared by premixing the two solids in chloroform, evaporating the solvent and, finally, dissolving the mixed solids in heptane at 10^{-5} M (Figure 11).

Upon mixing 10^{-4} M solutions of achiral "small" urea disk **2a** and chiral "small" urea disk **2b** a remarkable aggregate (Figure 11, squares) was formed just above room temperature (30−40 °C). Cotton effects opposite in sign and with intensities up to 5 times that of the pure chiral compound **2b** were observed. However, these initial aggregates (Figure 11, squares) proved not stable in time. After approximately 1 h, the Cotton

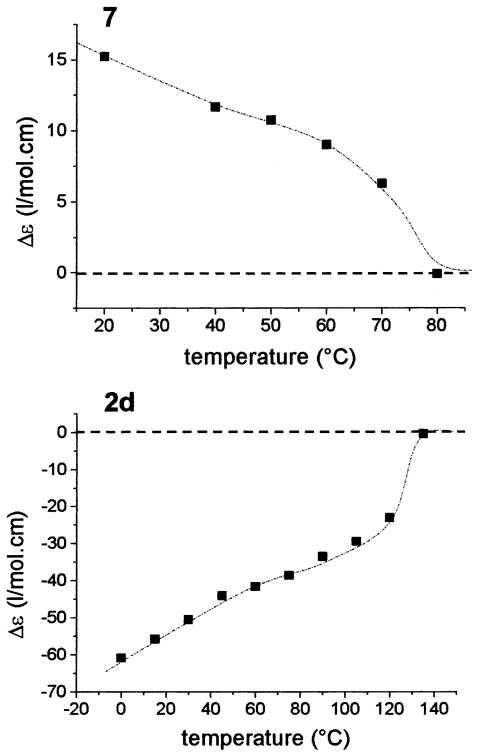

Figure 10. Temperature-dependent CD spectra of aggregates of "medium" di-urea **7** (upper graph) and tri-urea **2d** (lower graph) at $\lambda_{max} = 264$ and 275 nm, respectively (10^{-5} M in heptane for **7** and in dodecane for **2d**).

Table 8. Amplification of Chirality of Amides **1a**−**f** and Ureas **2a**−**f**; Hysteresis Indicates Whether Kinetic Factors Influence the System during Sample Preparation and Measurements[a]

compd	1a/b[b]	1c/d	1e/f[c]
amplification of chirality	40		40
hysteresis	no		no
compd	**2a/b**	**2c/d**	**2e/f**
amplification of chirality	5	2	no
hysteresis	yes	yes	

[a] **2a/b**: 10^{-4} M, all others: 10^{-5} M in heptane. [b,c] See the footnotes of Table 6.

effect changed completely (Figure 11, dots). More than 75% chiral compound gave the Cotton effect of the pure chiral compound **2b**, while less chiral compound gave no substantial Cotton effect.

Mixing Amides and Ureas. The above findings were confirmed when amide disks **1a**−**f** were mixed with urea disks **2a**−**f**. If amplification of chirality occurs upon mixing of a chiral amide with an achiral urea (or an achiral amide with a chiral urea), this would imply that amide and urea molecules can be accommodated in one single aggregate. Upon mixing in solution 5−20 mol % of "small" chiral amide **1b** with "small" achiral urea **2a** a chiral amplification of 4 was observed (Figure 12). However, within 1 h, the effect disappeared, and a linear relationship was observed similar to that found in the remainder of the concentration range (20−100 mol % **1b**). When solutions of "small" achiral amide **1a** and "small" chiral urea **2b** were mixed, no Cotton effect appeared.

Mixing "medium" disks **1d** and **2c** (chiral amide and achiral urea) or **1c** and **2d** (achiral amide and chiral urea) did not give rise to any Cotton effect, independent of the type of mixing. Upon mixing "large" disks **1f** and **2e** (chiral amide and achiral urea), or **1e** and **2f** (achiral amide and chiral urea), a linear relationship existed between the percentage of chiral compound and the intensity of the Cotton effect, implying that also "large" amide and urea disks are not compatible.

Discussion

From the results above, it is clear that all investigated disks form helical columnar structures in the solid (liquid crystalline) phase. Most of these C_3-symmetrical supramolecular architectures are retained in gels in apolar solution. For "medium" urea **2d** and "large" urea **2f**, respectively, the value for the cross section R_c of the molecule—and hence the supramolecular fiber—found in the AFM height profile (22 and 32 Å, respectively) corresponds well to the CPK estimate (20 and 32 Å, respectively). The values for the cross section R_c found with SANS, X-ray or "AFM-width" also correspond (Table 4, 33 and 40 Å, respectively), but are substantially larger than those found using AFM height profiles or CPK models. This can be explained because the latter two techniques are underestimating the space occupied by the aliphatic tails. In the case of CPK modeling, this was done consciously by only taking into account the aromatic core; in case of AFM height profiles, one can imagine that the AFM tip compresses the flexible outer shell of the fiber. Strikingly, the difference between the values found with CPK/AFM-height and AFM-width/X-ray/SANS is 10 Å, which corresponds to the space taken up by one extended chiral alkyl chain ((*S*)-3,4-dimethyloctyl: 8×1.25 Å $= 10$ Å). X-ray studies on systems as different as "large" amide **1f**[19] and sugar appended organogelators[3n], have shown that solvent molecules can widen the intercolumn distance by taking part in the supramolecular ordering. But in view of this striking difference of 10 Å, the influence of the solvent is most likely small in case of "medium" and "large" ureas **2d** and **2f**. This is confirmed by the value for the cross section R_c of **2f** found with SANS in the lyotropic phase (39 Å), that corresponds closely to that of **1f** found with X-ray for the neat compound (38 Å).

Surprisingly, "medium" amide disks **1c/d** do not retain their helical columnar structure in apolar solution, in contast to all the other amide and urea disks (**1a/b**−**e/f**, **2a**−**f**). The small liquid crystalline phase found for **1d** and the good solubility of **1c/d** can be indications for this behavior. "Medium" amide disks with inversed (nitrogen centered) amide groups do not form chiral aggregates either,[22] confirming the behavior found for "medium" amide disks **1c/d**. Generally, it depends on several factors whether aggregates are formed, among which, the strength of the hydrogen bonding, the strength of the $\pi-\pi$ and van der Waals interactions and the mutual proportionality of the two. Apparently, the combination of $\pi-\pi$ stacking between single aromatic rings and hydrogen bonding between amide groups is not strong enough to form helical stacks. In the "small" amide disks **1a/b**, strong van der Waals interactions probably account for a crystalline like packing of the alkyl tails. Moreover, chirality is easily expressed, because the distance of the chiral center to the chromophore (center of the molecule) is small. In the "large" amide disks **1e/f** strong $\pi-\pi$ interactions are present between the planarized and preorganizing bipyridinyl rings, which both stabilize the aggregate and cause chirality to be transferred a long way.

Strikingly, and in contrast to the "medium" amide disk **1d**, the "medium" urea disk **2d** does show supramolecular aggrega-

(22) To be published.

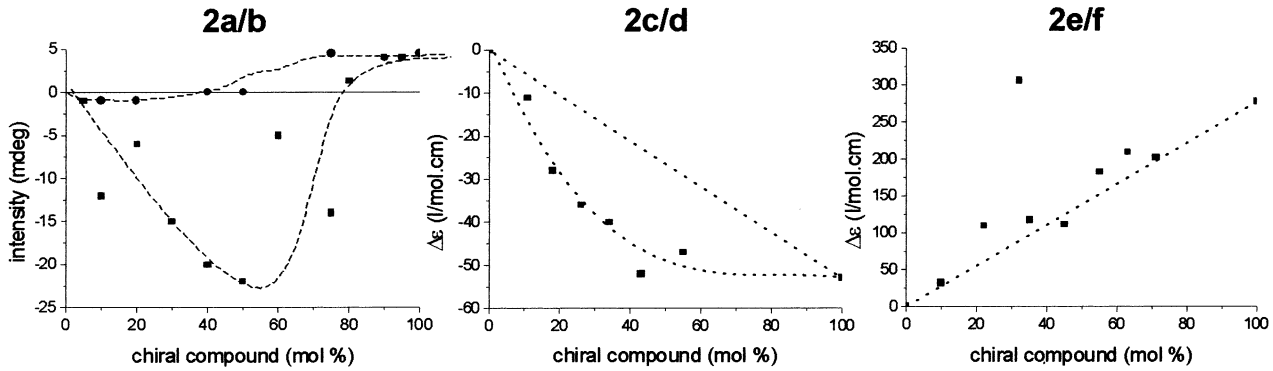

Figure 11. "Sergeants-and-soldiers" measurements of "small" **2a/b** (left), "medium" **2c/d** (middle) and "large" **2e/f** (right) urea disks at λ_{max} = 228, 275 and 295 nm, respectively (**2a/b**: 10^{-4} M, **2c/d** and **2e/f**: 10^{-5} M in heptane).

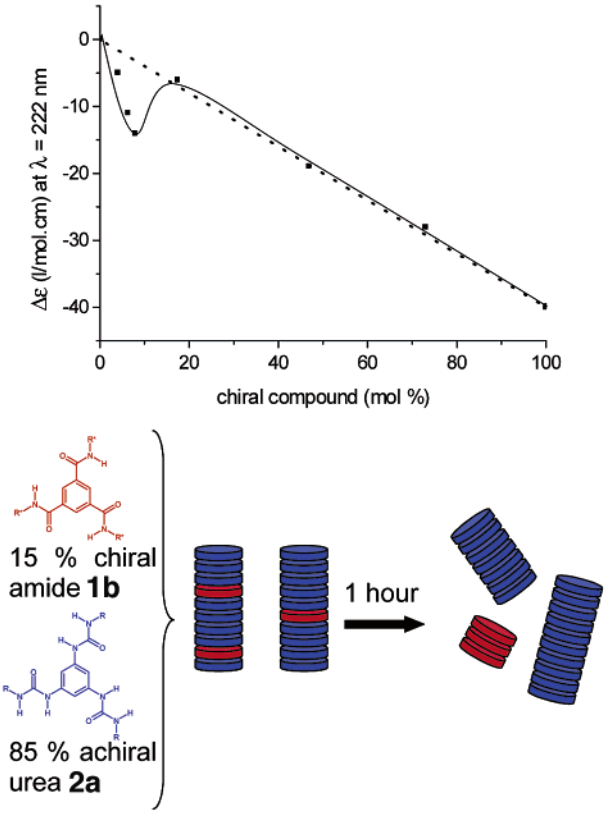

Figure 12. "Sergeants-and-soldiers" measurements with "small" chiral amide **1b** and "small" achiral urea **2a** (5×10^{-5} M in heptane). The schematic representation shows the mixing of "small" disks. Mixing 15% of chiral amide **1b** (red) and 85% of achiral urea **2a** (blue) gives aggregates containing both kinds of disks (red and blue). However, in time the disks rearrange into two different stacks, containing only chiral amide **1b** (red) or only achiral urea **2a** (blue).

tion in solution. Apparently, in this case 'stronger' intermolecular hydrogen bonding increases the tendency to form chiral aggregates. The CD effect produced by "small" urea **2b** is only marginal, also compared to that of "small" amide **1b**. This is in congruence with IR and gelation experiments, which show that toluene is clearly a better solvent for aggregation of urea **2b** than heptane, probably due to the very low solubility of **2b** in the latter solvent. However, CD measurements have to be performed in heptane, because of the overlap in absorption of toluene and "small" urea **2b**. The Cotton effect of "large" urea **2f** is comparable in intensity and shape to that of "large" amide **1f**, but opposite in sign, although both molecules are based on the same (*S*)-3,7-dimethyloctyl side chain, with the same (*S*)-configuration. The additional NH group in urea **2f** could cause an "odd−even" effect, inducing a sign inversion with every atom placed between the chiral center and (a part of) the chromophore. This odd−even effect has been observed before in the optical rotation of a series of poly(isocyanides)[23a] and polythiophenes.[23b] Alternatively, the additional NH group in urea **2f** could also slightly alter the conformation of the disk in the stack, inducing a small change in the pitch of the helix, which could suffice to change the sign of the Cotton effect produced by the helical aggregate.

Differences between amide and urea stacks become more evident when temperature-dependent CD behavior is studied. The temperature at which the Cotton effect disappears is significantly higher for "medium" urea **2d** (135 °C) than for "small" and "large" amides **1b** (90 °C) and **1f** (110 °C), indicating that the three additonal hydrogen bonding protons of the urea indeed can strengthen the supramolecular aggregate. Notably, the "large" urea disk **2f** (80 °C) cannot do so, implying that the aggregate of the "large" disk is less stable upon heating than that of the "medium" one **2d**. This can be rationalized by the fact that the intermolecular hydrogen bonds of the "large" urea **2f** might be weaker due to competitive intramolecular hydrogen bonding to the bipyridinyl groups. Furthermore, the reversible behavior of the amide molecules is in contrast with the hysteresis of 2 days for urea **2d** and 1.5 hours for urea **2f**. The amide molecules reach thermodynamical equilibrium immediately, whereas kinetics intervenes before the urea disks reach their thermodynamically controlled aggregation state. These findings were confirmed by comparing temperature-dependent measurements of mono-urea **6**, di-urea **7** and tri-urea **2d**. The one urea group of **6** does not have enough hydrogen bonding capacity to form chiral superstructures in solution. The reversible temperature-dependent behavior of di-urea **7** (80 °C) implies that the aggregate formed by its four hydrogen bonding protons is less rigid than the typical aggregate formed by tri-urea **2d** in which all six hydrogen-bonding protons are involved.

Knowing that the amide aggregates **1** behave much more flexibly and reversibly than the rigid urea stacks **2**, it is not surprising that the urea disks do not show the pronounced "sergeants-and-soldiers" effect, as that found in case of the amides. These "sergeants-and-soldiers" measurements are able to show clear differences between "formally" reversible archi-

(23) (a) Amabilino, D. B.; Ramos, E.; Serrano, J.-L.; Sierra, T.; Veciana, J. *J. Am. Chem. Soc.* **1998**, *120*, 9126−9134. (b) Ramos Lermo, E.; Langeveld-Voss, B. M. W.; Janssen, R. A. J.; Meijer, E. W. *Chem. Commun.* **1999**, 791−792.

tectures and systems with a nonequilibrium character. Furthermore, "sergeants-and-soldiers" measurements give valuable information about the compatibility of the constituting components (which might be largely different chiral and achiral molecules[19,9o]), especially when the (mixing) behavior of the ureas **2** is hard to study in the solid state (vide supra).

Where stacks of achiral and chiral molecules cannot be brought to compatibility in case of "large" ureas **2e/f**, "medium" urea disks **2c/d** can only be premixed in a good solvent. However, "small" urea molecules **2a/b** do mix in apolar solution, although, here also, kinetics plays an important role. The mixed stacks, consisting of achiral and chiral molecules, undergo microphase separation within an hour, giving aggregates containing either only chiral or achiral molecules. Therefore, in a solution containing both **2a** and **2b**, probably three types of aggregates are present (Figure 11, circles): aggregates consisting of chiral compound **2b** (giving a small, positive Cotton effect), of achiral compound **2a** (giving no Cotton effect), and aggregates consisting of both **2a** and **2b** (giving a negative Cotton effect), the latter being kinetically favored, the former two, thermodynamically favored. It is believed that the three methyl groups in chiral **2b** destabilize $\pi-\pi$ interactions between the disks in such a way that no ideal packing, such as the one in achiral **2a**, can be achieved.

Similar results and explanations apply to situations where "small" chiral amide **1b** and achiral urea **2a** are brought together in one solution. Also in this case, an aggregate in which both chiral and achiral disks are present is not thermodynamically stable and after microphase separation, two different columnar stacks are present containing either only chiral amide **1b** or achiral urea **2a** (Figure 12).

In the reverse case (mixing "small" chiral urea **2b** and achiral amide **1a**) the absence of a Cotton effect is rationalized by de marginal Cotton effect of pure chiral urea **2b**. Because "medium" amides **1c/d** are incapable of forming aggregates, let alone chiral ones, no amplification of chirality is to be expected upon mixing "medium" amide disks **1c/d** and ureas **2d/c**. Also the immiscibility of "large" amides **1e/f** and ureas **2f/e**, shows that amide and urea molecules are virtually immiscible. Obviously, a minor structural variation in the molecule (an extra methyl group or NH group) may dramatically disturb the subtle interactions between molecules building a helical columnar aggregate.

Conclusions

All C_3-symmetrical discotics investigated form helical, elongated, columnar aggregates, both in the solid (liquid crystalline) state and in solution (except for "medium" amide disks **1c/d**). This shows that a broad range of combinations of hydrogen bonding groups (amide and urea) and peripheral groups (alkyl, gallic, and bipyridinyl-gallic) is applicable wherein the formation of helical columns appears. AFM and SANS made it possible to visualize micrometer long strands consisting of thousands of molecules (2 μm for **2f**), displaying the enormous directionality of the hydrogen bonding interactions. These strands are held together by physical cross-link points, giving rise to gels with minimal gel concentrations as low as 1.2 mg/mL for **2a**.

However, choosing a different combination of secondary interactions may drastically affect the behavior and properties of the supramolecular aggregates. Substituting amide by urea results in a replacement of thermodynamics by kinetics. Temperature-dependent CD measurements show that, unlike the reversible behavior of the amide disks, distinct hysteresis takes place upon heating and cooling samples of ureas. Furthermore, the urea compounds do not display overwhelming "sergeants-and-soldiers" effects. This indicates that the initially formed, less-defined urea stacks only slowly transform into the well-defined, thermodynamically most favorable state. Once this optimal structure is found, the stacks have rigid rod character, which prevents the molecules from easy rearrangement and intermixing, as occurs in the amide stacks. In case of "medium" urea **2d**, a true rigid rod is formed, of which the constituting disks almost have to be destroyed (135 °C), before breaking up of the aggregates occurs. Changes in the van der Waals and $\pi-\pi$ interactions in the periphery of the molecule may strongly influence the capacity for aggregation (in case of **1c/d**). However, these influences are still hard to assess, because other factors, like the solubility and the distance of the chiral center to the chromophore, are altered simultaneously. The distinct influence of minor structural variations also accounts for the immiscibility of the amide and urea compounds, both forming similar C_3-symmetical supramolecular architectures, but in their own distinct way.

The exciting observation of intermediate stages within the formation of the urea helical aggregates can be interpreted as the folding of a supramolecular polymer, using its self-healing properties to reach or retain its most favorable conformation.[1b−c,6] The mobility of the disks in the helical architectures, leading to continuous reorganization and therefore the possibility of self-repair, are currently investigated in more detail.

Acknowledgment. We highly appreciate the support from the Institut für Werkstoffforschung at the GKSS Forschungszentrum in Geesthacht where Ralf Kleppinger performed SANS measurements. We thank Joost van Dongen and Xianwen Lou for MALDI-TOF/MS measurements and Henk Eding for elemental analyses. Furthermore, Daan Wouters is acknowledged for AFM pictures and Jolanda Spiering for the synthesis of various gallic acid derivatives.

Supporting Information Available: Experimental details concerning the techniques used (AFM, SANS), synthetic procedures and characterization data of all new compounds. This material is available free of charge via the Internet at http://pubs.acs.org.

JA020984N